J. Biochem. **141,** 535–544 (2007)
doi:10.1093/jb/mvm055

Structure of the Antitumour Enzyme L-Methionine γ-Lyase from *Pseudomonas putida* at 1.8 Å Resolution

Daizou Kudou[1], Shintaro Misaki[2], Masao Yamashita[1], Takashi Tamura[1], Tomoaki Takakura[3], Takayuki Yoshioka[4], Shigeo Yagi[5], Robert M Hoffman[5], Akio Takimoto[3], Nobuyoshi Esaki[6] and Kenji Inagaki[1,*]

[1]Department of Biofunctional Chemistry, Graduate School of Natural Science and Technology, Okayama University, Okayama-shi, Okayama 700-8530, Japan; [2]Diagnostic Division, Shionogi & Co., Ltd 2-5-1 Mishima, Settsu, Osaka 566-0022, Japan; [3]Discovery Research Laboratories, Shionogi & Co., Ltd 1-3, Kuise Tarajima 2-chome, Amagasaki, Hyogo 660-0813, Japan; [4]Strategic Development Department Development Division, Shionogi & Co., Ltd 12-4 Sagisu 5-chome, Fukushima-ku, Osaka 553-0002, Japan; [5]AntiCancer Inc., 7917 Ostrow Street, San Diego, CA 92111, USA; and [6]Institute for Chemical Research, Kyoto University, Uji, Kyoto 611-0011, Japan

Received October 2, 2006; accepted January 30, 2007; published online February 8, 2007

L-Methionine γ-lyase (EC 4.4.1.11, MGL_Pp) from *Pseudomonas putida* is a multi-functional enzyme, which belongs to the γ-family of pyridoxal-5′-phosphate (PLP) dependent enzymes. In this report, we demonstrate that the three-dimensional structure of MGL_Pp has been completely solved by the molecular replacement method to an *R*-factor of 20.4% at 1.8 Å resolution. Detailed information of the overall structure of MGL_Pp supplies a clear picture of the substrate- and PLP-binding pockets. Tyr59 and Arg61 of neighbouring subunits, which are strongly conserved in other γ-family enzymes, contact the phosphate group of PLP. These residues are important as the main anchor within the active site. Lys240, Asp241 and Arg61 of one partner monomer and Tyr114 and Cys116 of the other partner monomer form a hydrogen-bond network in the MGL active site which is specific for MGLs. It is also suggested that electrostatic interactions at the subunit interface are involved in the stabilization of the structural conformation. The detailed structure will facilitate the development of MGL_Pp as an anticancer drug.

Key words: L-methionine γ-lyase, pyridoxal 5′-phosphate, X-ray structure.

Abbreviations: AAT, aspartate aminotransferase; CBL_Ec, L-cystathionine β-lyase from *E. coli*; CGL, L-cystathionine γ-lyase; CGS_Ec, L-cystathionine γ-synthase from *E. coli*; MGL_Bl, L-methionine γ-lyase from *B. linens*; MGL_Cf, L-methionine γ-lyase from *C. freundii*; MGL_Eh, L-methionine γ-lyase from *E. histolytica*; MGL_Pp, L-methionine γ-lyase from *P. putida*; MGL_Td, L-methionine γ-lyase from *T. denticola*; MGL_Tv, L-methionine γ-lyase from *T. vaginalis*; PEG, polyethylene glycol; PLP, pyridoxal 5′-phosphate.

Pseudomonas putida lacks the reverse transsulphuration pathway (*1*). Instead, methionine is directly converted to methanethiol by L-methionine γ-lyase (MGL) which is then oxidized to methanesulphonate. MGL is therefore an essential enzyme for methionine metabolism in *P. putida* (*2*).

MGL catalyses the α,γ-elimination of L-methionine to α-ketobutyrate, methanethiol and ammonia (Eq. 1) (Scheme), as well as γ-replacement of L-methionine and various thiols (Eq. 2). α,β-Elimination and β-replacement of *S*-substituted L-cysteines are also catalysed by MGL (Eqs. 3 and 4, respectively).

This enzyme has been found in several microorganisms such as *P. putida, Trichomonas vaginalis, Entamoeba histolytica, Aeromonas* sp., *Citrobacter freundii, Brevibacterium linens, Porphyromonas gingivalis* and *Treponema denticola* (*3–10*). MGL has not been found in yeast and mammals. MGL has low sequence homology and high structure homology to other γ-family enzymes.

MGL has demonstrated antitumour efficacy in a number of methionine-dependent cancer cell lines including lung cancer, colon cancer, kidney cancer, brain cancer, prostate cancer, melanoma and fibrosarcoma (*11–15*). However, the stability of MGL_Pp in plasma is affected by: [1] immunogenicity, [2] proteolysis, [3] oxidation of the active site residues, [4] release of PLP and [5] instability of the active dimer. Modification of this enzyme with polyethylene glycol (PEG) has reduced immunogenicity and possibly inhibited proteolytic enzymes that could degrade MGL (*16*). PEGylated MGL is being developed as a cancer drug (*17–19*) and detailed structural information could greatly facilitate its development.

In a previous report (*20*), the overall crystal structure was reported with relatively high-resolution. However, the structural information of the N-terminal domain still was incomplete (residues 42–63) because of ambiguous electron densities. Recently the crystal structure of MGL from *Citrobacter freundii* (MGL_Cf) and *Trichomonas vaginalis* (MGL_Tv) was solved at 1.9 (*21*) and 2.2 Å resolution, respectively. The similarity of the tertiary structure of each subunit between MGL_Pp and MGL_Cf has been confirmed. The dimer and dimer–dimer

*To whom correspondence should be addressed. Tel/Fax: +81-86-251-8299, E-mail: kinagaki@cc.okayama-u.ac.jp

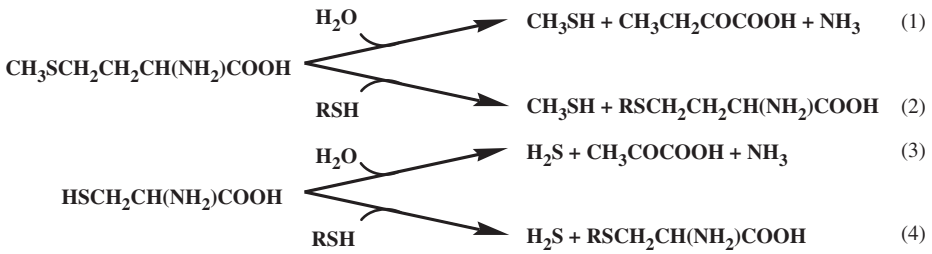

Scheme. MGL catalyzes α,γ-elimination, α,β-elimination, γ-replacement, and β-replacement reactions on L-methionine and L-cysteine, respectively

interactions, however, were merely mentioned and not described. In the present study, the crystal structure of MGL_Pp has been fully determined with geometrical information around the active centre as well as the N- and C-terminals. The interaction of the homodimer and homotetramer of MGL also has been revealed.

MATERIALS AND METHODS

The gene encoding MGL from *P. putida* ICR3460 was used in this study. The expression plasmid pMGL1204 and recombinant *Escherichia coli* were prepared as previously described (*22*). Production of recombinant MGL was performed as described in Takakura *et al*. (*23*). Recombinant *E. coli* was cultured in a jar fermentor and harvested at 28°C. The bacterial pellet was disrupted with a Manton Gaulin homogenizer (model 30CD, APV Gaulin GmbH, Lubeck, Germany). Recombinant MGL was purified to electrophoretic homogeneity in a three-step procedure consisting of polyethylene glycol treatment, followed by anion exchange chromatography using a DEAE-Sepharose FF column (Amersham Bioscience), and finally gel filtration using Sephacryl S-200 HR (Amersham Bioscience). MGL was detected by the activity assay described by Takakura *et al*. (*22*). One unit of activity is defined as the amount of MGL that catalysed the formation of 1 μmol of α-ketobutyrate per minute at 37°C.

Directed mutagenesis was performed on pMGL1204 using a pair of oligonucleotide primers, containing a point mutation. Primers used are shown in Table 1. After PCR amplification, expression plasmids containing the desired mutations were identified by sequencing of both strands. Production and purification of MGL mutant enzymes were performed as described earlier except without the gel filtration step.

The enzyme was crystallized using the sitting drop method at 4°C. Prior to crystallization the enzyme was extensively dialysed against a 50 mM sodium phosphate buffer solution, pH 7.2 with a combination of 40% MPD, 30% PEG6000 and 1% ammonium sulphate as precipitants. A 10 μl drop comprising equal volumes of the reservoir solution and a solution of 32.7 mg/ml protein in 10 mM sodium phosphate (pH 7.2) and 0.5 mM PLP was kept at 4°C. The crystal was grown to a size of up to $0.5 \times 0.5 \times 0.5\,mm^3$. Diffraction data were obtained with synchrotron radiation [BL24XU (Hyogo Prefecture beamline)] at SPring-8 using RAXIS IV (Rigaku). Data were processed and scaled with the DENZO and SCALEPACK software package. Crystal data and data statistics are summarized in Table 2. This crystal contains one tetramer in the asymmetric unit. The crystal structure was solved by the molecular replacement method using the dimer structure of L-cystathionine β-lyase (CBL) as a starting model with the X-PLOR software package. Model building was

Table 1. **Primers used in this study.**

Mutation	Sequence (5′ to 3′)
R61A	CCGGGCATTTCTACAGCGCCATCTCCAACCCCACC
R61E	GCCGGGCATTTCTACAGCGAAATCTCCAAC CCCACCCTC
R61F	CCGGGCATTTCTACAGCTTCATCTCCAACCCCACC
L341H	CGCGCGGTGAGCCATGGCGATGCCGAG
F128C	GGCATCGGCGAGTGCGGGGTCAAGCTG
S248C	CGGTGCGGTGCTCTGCCCCCATGACGCCG
D385C	CTGGAAGACATCGACTGCCTGCTGGCCGATGTG
G9C	CCAACAAGCTCCCATGCTTTGCCACCCGCG
C116S	CAACACCCTGTACGGCAGCACCTTTGCCTTC
C116T	GCAACACCCTGTACGGCACCACCTTTGCCTTCCTG

Table 2. **Data collection and refinement statistics.**

Space group	$P4_32_12$
Unit cell dimensions (Å)	$a = b = 133.13$, $c = 215.24$
Wavelength (Å)	0.8340
Resolution range (Å) (highest resolution shell)	40.0–1.80 (1.86–1.80)
Mosaicity	0.504
Reflections	
Observed	781,757
Unique	176,570
Completeness	98 (89)
Redundancy	4.41 (2.65)
I/σ (I)	8.2 (6.1)
R_{merge} (%)	7.50 (42.7)
Number of protein atoms included in refinements	12056
R_{cryst} overall (%)	20.4 (24.3)
R_{free} (%)	22.4 (27.3)
Water molecules	1091
R.M.S deviations from ideality	
Bond length (Å)	0.018
Angles (°)	1.525
Ramachandran plot	
Most favourable regions (%)	91.4
Allowed regions (%)	7.9
Disallowed regions (%)	0.9

performed on the Turbo-Frodo graphic program and structure was refined by X-PLOR. The final *R*-value was 20.4% (R_{free} = 22.4%). The density map shows that the active site is composed of a homodimer and the N-terminus and C-terminus are also visible. The coordinates of this crystal structure have been deposited in the Protein Data Bank under ID code 2O7C. Coordinates of MGL_Tv, MGL_Cf, CBL_Ec and CGS_Ec (CBL and CGS from *E. coli*) were obtained from the RCSB Protein Data Bank with internal codes 1E5F, 1Y4I, 1CL1 and 1CS1, respectively.

RESULTS AND DISCUSSION

Overall Structure—The overall tetramer structure of MGL_Pp (Fig. 1a) is highly similar to the closely related CBL_Ec (*24*), a feature that was utilized in the molecular-replacement structure determination. MGL_Pp is known to exist as an α_4-tetramer in solution. The monomer folds-up into three spatially and functionally distinct regions: (1) an extended N-terminal domain (residues 1–63) that includes two helices and three β-strands, (2) a large PLP-binding domain (residues 64–262), which comprises a mainly parallel seven-stranded β-sheet that is sandwiched between eight α-helices and (3) a C-terminal domain (residues 263–398) (Fig. 1b). The view of residues 42–63 of this enzyme supplies new aspects to the subunit interactions. In the N-terminal arm, residues 1–39 are mainly concerned with stabilization of the dimer–dimer interaction. Residues 34–63 stabilize dimer formation (active dimer), and contain some important residues that comprise the active site. Below, we show that there is a highly significant correlation between the N-terminus region and the PLP-binding domain of the neighbouring subunit.

The two monomers associate tightly to form a dimer as shown in Fig. 2 which is the known active dimer. The compact monomer shape is achieved by packing the PLP-binding domain against the C-terminus. An extended N-terminus protrudes from the bulk of the subunit, forming a clamp to the neighbouring monomer similar to other γ-family enzymes (Fig. 2a). The intimate binding between the two monomers in the dimer is established by several hydrogen bonds, hydrophobic interactions and most remarkably, by various intermolecular active-site interactions. The phosphate group of PLP interacts strongly with Arg61* (the asterisk, henceforth, indicates a residue from the adjacent subunit of the active dimer) of the N-terminal part of the adjacent subunit which corresponds to Arg58* in CBL_Ec. A similar interaction is made by Tyr59* which is one of the donors in the hydrogen-bonding network around the PLP phosphate.

In the centre of the dimer, near the active site, three helices and one loop are in close contact with each other and with their symmetry mates. Hydrophobic residues are mostly found in the contact region of these helices and in a loop, forming a large hydrophobic region comprising residues Trp98 and Ala245. Thus, the dimer is required for the catalytically active enzyme.

The tetramer is formed by symmetric association of two dimers, resulting in an overall non-crystallographic 222 symmetry. The MGL tetramer interface is larger than the interfaces of other PLP-dependent enzyme structures.

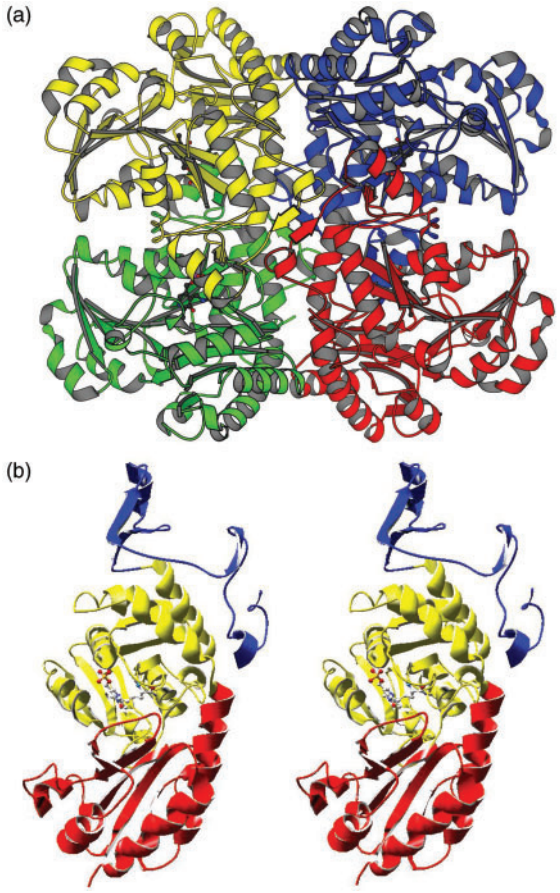

Fig. 1. **Overall fold of the MGL_Pp.** (a) The homotetramer is built-up as a dimer of active dimers, resulting in an overall 222 symmetry. The individual monomers are colour-coded. The PLP cofactor is mainly linked by the central domain, held in a ball and stick presentation. (b) Stereo ribbon presentation of the MGL monomer. The N-terminal domain is held in blue, the PLP-binding domain in yellow and the C-terminal domain in red. PLP and PLP-binding Lys211 are shown in a ball and stick representation.

The N-terminus is very important for the formation of the dimer and the dimer–dimer interface (Fig. 2). Therefore, the conformation of the dimer structure is essential for the binding of PLP to the apoenzyme, as is typical of this subclass of vitamin B_6-dependent enzymes. It is deduced that the structure of the active dimer would be stabilized by the formation of the tetramer. The above quaternary association leads to the formation of four active sites per tetramer, two made up within each active dimer. These two active sites are quite close to each other. For several enzymes of the γ-family, evidence has been obtained suggesting that only one active site per dimer is actually operating or being inhibited by mechanism-based inactivators (*25*).

Active Site—The active site design is shown schematically and spatially in Fig. 3. In the cleft formed between the two domains of the subunit at the dimer interface, there is strong electron density adjacent to a conserved lysine residue, corresponding to a bound pyridoxal phosphate molecule. PLP is covalently attached to MGL via the ε-amino group of Lys211, a residue located at the

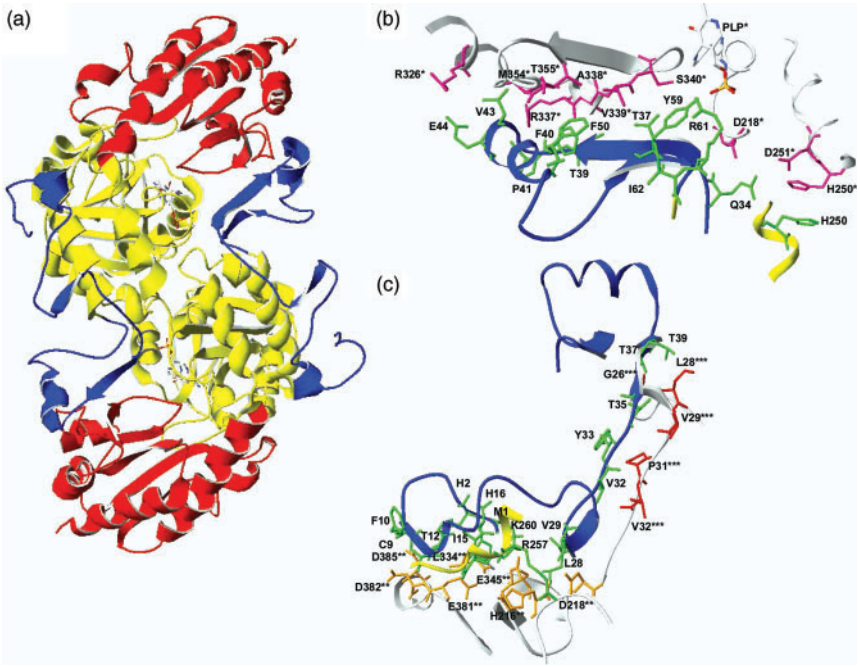

Fig. 2. **Active dimer of MGL_Pp viewed along the non-crystallographic 2-fold axis.** Note that the N-terminal domain of one subunit is part of the active site of the neighbouring monomer. (a) Ribbon presentation of the MGL dimer. Two monomers share active-site residues *via* their N-terminal domains (blue). (b) The interaction of the interface with each monomer. Amino acids are labelled with one-letter code and MGL numbering. The residues from the first subunit are green and the residues from the second subunit are red with an asterisk. (c) The interface between the active dimers. Orange residues with double asterisk are from the third subunit and red residues with triple asterisk are from the fourth subunit.

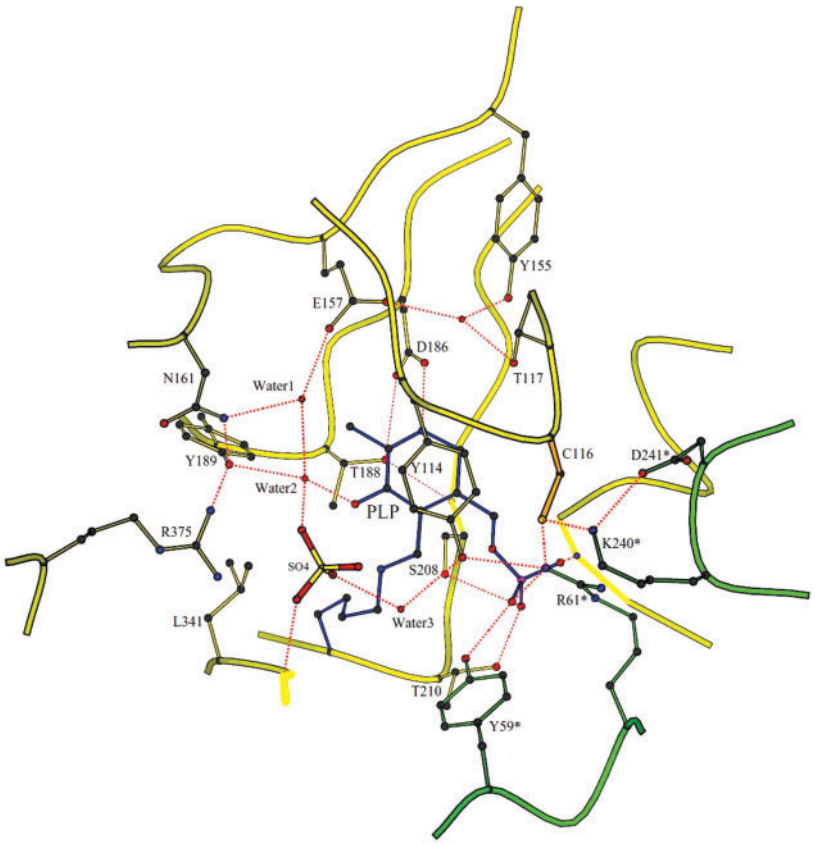

Fig. 3. **Geometry of active site in MGL_Pp.** Peptide portions from the two different MGL monomers forming the active dimer are colored yellow and green. Active site residues are identified as discussed in the text.

loop between the two β-strands. The pyridine nitrogen atom (N1) of PLP forms a strong hydrogen bond/salt bridge (2.73 Å) with the carboxylate group from Asp186 which stabilizes its positive charge and increases the electrophilic character of the cofactor. The carboxylate group of Asp186 forms a strong hydrogen bond with the hydroxyl group of Thr188. Asp186 and Thr188 are largely conserved in the α- and γ-families of PLP-dependent enzymes. These hydrogen bonds fix the Asp186 carboxylate group in a geometrically optimal position for interaction with the N1 of PLP. Furthermore, the hydrogen bonds which originate from Asp186 should permit charge dissipation during the catalytic cycle into the protein periphery, stabilizing the quinonoid intermediate similar to Asp230 in 1-aminocyclopropane-1-carboxylate synthase (ACCS) and Asp222 in AATase (*26*).

The methyl group at C2 of the cofactor is not involved in any specific interactions with the protein. The presumably ionized hydroxyl group at C3 receives only one weak hydrogen bond from a well-ordered water molecule in the active site of MGL. The positive charge of the nitrogen of the Schiff base is stabilized by interaction with the deprotonated hydroxyl group at C3.

At position 4, the original PLP aldehyde function has reacted with the side chain of Lys211 to form the internal aldimine. The aldimine is protonated, based on the strong absorbance of the crystals near 425 nm.

Besides the covalent bond, the cofactor is anchored predominantly in the active site through its phosphate group at position 5, for which eight hydrogen bonds to the protein residue are discernible, to the main chain amide nitrogens of Gly89 and Met90 which lie at the N-terminus of α4 helix, and to the side chains of Ser208, Thr210, Tyr59* and Arg61*. Ser208 and Thr210 lie at the same loop as Lys211. The phosphate group of PLP interacts strongly with Arg61* of the N-terminal part of the adjacent subunit the same as Arg58* in CBL_Ec (*24*). A similar interaction is made by Tyr59* which is one of the hydrogen donors in the hydrogen-bonding network around the PLP phosphate. Arg61*, which lies at the N-terminus of the βc strand, is the hydrogen donor for four hydrogen bonds. Thus, Arg61* should compensate directly for the negative charges of the phosphate group. Furthermore, Arg61* also interacts with the ring-stacking Tyr114 hydroxyl group which is only observed within this group of PLP enzymes, suggesting a functional role for the Arg61*-Tyr114 interaction.

The pyridine ring is sandwiched between Tyr114 and Thr188/Ser208 which impedes any vertical movements of the cofactor with respect to the pyridine ring plane. The latter two residues are in van der Waal's contact with all ring atoms of the pyridine ring, minimizing movement of the cofactor in that direction. The phenol ring of Tyr114 is located at an angle of about 10° with respect to the pyridine ring. Apart from restraining the cofactor, the resulting ring-stacking interaction should, in analogy to the situation in L-cystathionine γ-synthase (*27*), increase the electron-sink character of the cofactor. The interaction of MGL-Tyr114 is known to be essential to the mechanism of AAT-Trp140 (*28*).

It is interesting to compare the pocket of the substrate in a structural comparison between MGL_Pp and CBL_Ec using the suicide inhibitor aminoethoxyvinylglycine (1CL2) or with MGL_Tv using the suicide inhibitor propargylglycine (1E5E). The carboxyl group of the suicide substrate in the active site makes two hydrogen bonds with the guanidinium group of Arg372 in CBL_Ec; Arg362, in CGS_Ec and Arg373 in MGL_Tv. In MGL_Pp, Arg375, which makes a hydrogen bond to the hydroxyl group of Tyr189, corresponds to the Arg residues described earlier in the other enzymes. This residue is largely conserved in most of the α- and γ-families of PLP-dependent enzymes. Accordingly, this arginine residue is assumed to bind the α-carboxylate group of the incoming substrate.

As for the reaction specificity of MGL for L-methionine, it is thought that electrostatic force, any steric hindrance and the hydrophobicity of residues at the active centre would be essential factors for the recognition of the substrate from comparison of the active-site geometries between MGL_Pp and other PLP-dependent γ-family enzymes. First, a hydrogen bond network or electron transfer would more likely contribute to the reaction specificity of the substrate such as the hydrogen-bond network between Tyr114, Cys116, Lys240* and Asp241*. These residues are conserved in most heterologous MGLs. Tyr114, which lies at the N-terminus of the helix α5, plays a role as a general acid catalyst in the elimination of the γ-substituent of the substrate (*29*). Cys116, which lies on the helix, is a possible nucleophilic residue, identified by chemical modification with a thiol-specific cyanylating reagent, 2-nitro-5-thiocyanobenzoic acid (NTCB) (*30*). However, the sulfhydryl group of this residue is not directly required for the enzyme's catalytic role. Lys240*, Asp241* and Arg61* from the adjacent subunit make a hydrogen bond/salt bridge with each other (Fig. 3). Moreover from the results of mutagenesis experiments targeting Cys116, it is concluded that this hydrogen-bond network, consisting of Tyr114, Cys116, Lys240* and Asp241*, is important for substrate selectivity for L-methionine.

In addition to Tyr114, Cys116 and Arg375, hydrophobic residues (Phe58*, Ile62*, Ala119, Leu236 and Val339) play an important role for substrate recognition, instead of charged residues in CGS, CBL and CGL (*31*). Asp45*, Arg49* and Glu325 of CGS_Ec, which contact the cysteinyl functional group of the α carbon of the substrate, are substituted with hydrophobic residues Phe58*, Ile62* and Val339, respectively, in MGL_Pp. Arg106 of CGS_Ec, which contacts the distal carboxyl group of *O*-succiny-L-homoserine, is substituted with Ala119 in MGL_Pp. Glu235 of CBL_Ec, which forms an ion pair with Arg59* anchoring the phosphate group of PLP and contacts the distal amide group of cystathionine, is substituted by Leu236 in MGL_Pp. Thus, in MGL_Pp a hydrophobic patch operates as the recognition site for the side chain of the methionine substrate.

Conversion of Residues—Site-directed mutagenesis was carried out as described above (Materials and Methods section). Based on the structural information on MGL_Pp, several mutants were made to observe the change in γ-elimination activity on L-methionine and L-homoserine. Point mutations, indicated in parentheses, are related to the following: (a) tetramer formation

(D385C and G9C), (b) dimer formation (F128C and S248C), (c) PLP interaction at the active site (R61A, R61E, R61F and L341H) and (d) hydrogen-bond network in the active site (C116S and C116T). Specific activities of all mutants were expressed as a percentage of the wild-type activity which was considered to be 100% (Table 3). The calculated specific activity for the wild-type enzyme was 61.2 units/mg. First, for purpose of stabilization of active dimer, we tried to introduce the S–S bond linkage into the interface. Phe128 and Ser248, which are very close to each other, lie in close proximity at the interface of the active dimer. Mutation (F128C and S248C) of these residues caused activation of enzyme activity (12 and 31% higher than wild type, respectively). Asp385 and Gly9 are the closest residues at the dimer–dimer interface, and Asp385 makes a strong hydrogen bond to the side chain of Thr12. In this regard the D385C-G9C double mutant decreased the activity. Each cysteine mutant was dialysed in buffer without dithiothreitol. These oxidized enzymes showed the same relative activity as the wild-type enzyme (data not shown). It is assumed that there are no S–S bond linkages in the mutants. These results suggested that at the subunit interface electrostatic interactions are important for structural flexibility.

Next, we examined the active-site residues. All Arg61 mutants lost activity, suggesting that this residue is very important to the catalytic activity. Around PLP, most residues which comprise the active site are conserved in γ-family enzymes. Leu341, which lies at a position where the α-carboxylate of the substrate should be bound, is highly conserved in the γ-family enzymes except CBL_Ec. Therefore, it is not surprising that L341H also lost activity. Cys116 is located at the active centre in MGL_Pp. Both C116S and C116T mutants lost activity. In most mutants, the M/H ratio (α,γ-elimination activity ratio) was the same as that of wild type. However, differences in the ratio of C116S and C116T were detected. Compared with L341H and D385C-G9C, which lost activity on both substrates, the decrease of the M/H ratio for C116S and C116T suggests that Cys116 is involved in substrate specificity.

In summary, the tetramer functions to maintain an active dimer. The residues around PLP are well optimized for each reaction. The substrate specificity of MGL appears to be due to Cys116. A more detailed study of Cys116 should yield information on the mechanism of substrate recognition in MGL_Pp.

Interface of the Homodimer—Dimer formation is stabilized by an extended turn in the N-terminal arm (Fig. 2b). The N-terminal turn (residues 34–62) including Gln34, Thr37, Thr39, Phe40, Pro41, Val43, Glu44, Phe50, Tyr59, Arg61 and Ile62 and C-terminal domain of one partner monomer make important interactions that are required for proper structure, and mostly allow hydrophobic interactions. The N-terminus region, which is involved in dimer interaction, is also part of the active site. Phe58 and Ile62 are engaged in substrate recognition with hydrophobic interaction with the side chain of the substrate. Furthermore, the hydrogen bonds between the βb and βc strands enable the region to be more stable, Tyr59 and Arg61 strongly and moderately, respectively, connect with the phosphate of PLP. The stacking interaction of the imidazole ring of His250 from each subunit is also involved in dimer interaction. We propose that dimer stabilization in the active dimer is important for the catalytic cycle.

Table 3. **Relative activity of wild type and mutants of MGL_Pp on L-methionine.**

	Relative activity (%)	M/H ratio
Native	100	41.3
R61A	1	N.D
R61E	0	N.D
R61F	2	N.D
L341H	9	52.0
F128C	112	42.5
S248C	131	51.6
D385C-G9C	46	44.2
C116S	9	3.7
C116T	40	17.3

Note: N.D: not determined; *M*/*H* ratio: the rate of γ-elimination activity on L-methionine and L-homoserine.

Interface of the Homotetramer—The interface between the active dimers in the homotetramer of MGL_Pp comprises N-terminus residues including Met1, His2, Gly9, Phe10, Ala11, Thr12, Ile15, His16, Gly26, Leu28, Val29, Val32, Tyr33, Thr35, Thr37 and Thr39; PLP-binding domain residues including His216, Asp218, Arg257 and Lys260 and C-terminus residues including Leu334, Ser336, Glu345, Glu381 and Asp385 of one monomer (Fig. 2c). The interface of each dimer consists mostly of electrostatic interactions. It is important for stability that charged residues have a partner with the opposite charge, and that repulsive or unfavourable contacts are minimized. The hydrogen bond between Arg257 and Asp218* is strongly associated with dimer–dimer formation and the stabilization of the aldimine formation at the active site, because Asp218 lies in the same loop (βi–βj loop) as does Lys211. Moreover, these residues are highly conserved in γ-family enzymes. The tetrameric structure is mostly stabled by the hydrogen-bond linkages of the dimer–dimer interface; however, there is no evidence that there are functional interactions.

Comparison with Other γ-Family Enzymes—Inoue *et al*. (*32*) cloned the *mgl* gene from *P. putida* and compared it with the other γ-family enzymes. Their results indicated that the five different enzymes of the transsulphuration and direct sulphydrylation pathways are highly similar in 3D structure. Furthermore, Motoshima *et al*. (*20*) also found sequence similarities between MGL_Pp and other γ-family enzymes such as MGL_Tv, CBL_Ec and CGS_Ec. Extensive sequence information on MGL enzymes is now available. The sequences vary in length from 389 to 425 amino acids. The protein sequence alignments (ClustalW) of MGL_Pp with MGL from *T. denticola*, *C. freundii*, *T. vaginalis*, *E. histolytica* and *B. linens* are illustrated in Fig. 4.

The alignment indicates that the PLP-binding domain and C-terminal domain exhibit especially high homology. In contrast, the homology in the N-terminal part is low.

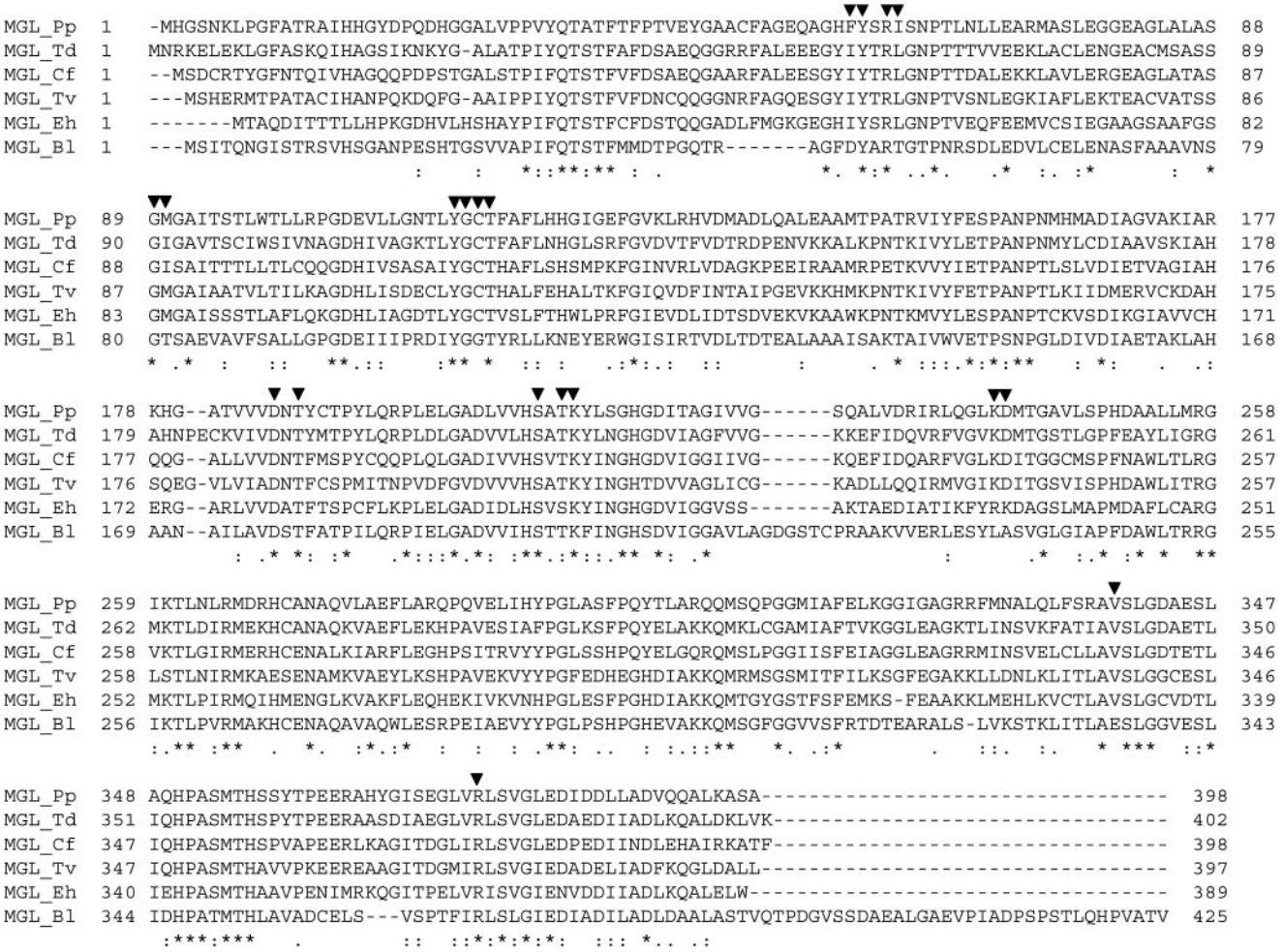

Fig. 4. **Sequence-based alignment of heterologous MGLs.** Abbreviations used: MGL_Pp, MGL from *P. putida*; MGL_Td, MGL from *T. denticola*; MGL_Cf, MGL from *C. freundii*; MGL_Tv, MGL from *T. vaginalis*; MGL_Eh, MGL from *E. histolytica* and MGL_Bl, MGL from *B. linens*. Conserved residues are shown with asterisks, homologues with dots and colons. Arrows point to active-site residues.

Residues involved in cofactor binding (Tyr59, Arg61, Gly89 and Asp186) and catalysis (Tyr114, Lys211 and Arg375), which were previously shown to be essential, are invariant.

Cys116 has been thought to be essential for catalysis. This residue is mostly conserved in heterologous MGLs. However, MGL from *B. linens* (MGL_Bl), which has a longer amino-acid sequence, does not have the cysteinyl residue at the active site, but a glycyl residue instead (*33*). Although the properties of MGL_Bl, such as substrate specificity and enzyme inhibition, are similar to the other MGL enzymes, the α,γ-elimination activity on L-methionine of MGL_Bl has a 6-fold higher K_m than that of MGL_Pp, suggesting the importance of the cysteinyl residue.

An alignment based on secondary structure (Fig. 5) reveals that most elements of secondary structure were conserved within the γ-family enzymes. One of the remarkable differences in this point is the N-terminal structure, suggesting that the diversity of each N-terminus contributes recognition for each natural substrate. MGL_Pp has two α-helices and three β-strands which are barely similar to those of MGL_Tv, MGL_Cf, CBL_Ec or CGS_Ec (Fig. 6). The secondary structure of the N-terminus of MGL_Pp is specific to the γ-family of enzymes. The first loop (residues 1–9) is longer than those of CBL_Ec and CGS_Ec. The first helix (α1) is conserved in each enzyme. The first strand (βa) is conserved in CGS_Ec and the second strand (βb) is not conserved in CBL_Ec and MGL_Cf. The second helix (α2) is not conserved in CGS_Ec. The third strand (βc) is specific to MGL_Pp and MGL_Tv. This strand is located at the vicinity of the active site of the neighbouring subunit in the dimer, restricting the movement of the phosphate group of PLP. The hydrogen-bond linkage between two strands in the N-terminus, βb and βc, has an effect on the stability and the flexibility of the N-terminal domain. This β-sheet is characteristic of MGL_Pp and MGL_Tv.

CONCLUSION

MGL is a tetramer, built up as a dimer of dimers (Fig. 1a). Although there is little significant sequence homology between MGL_Pp and other γ-family enzymes

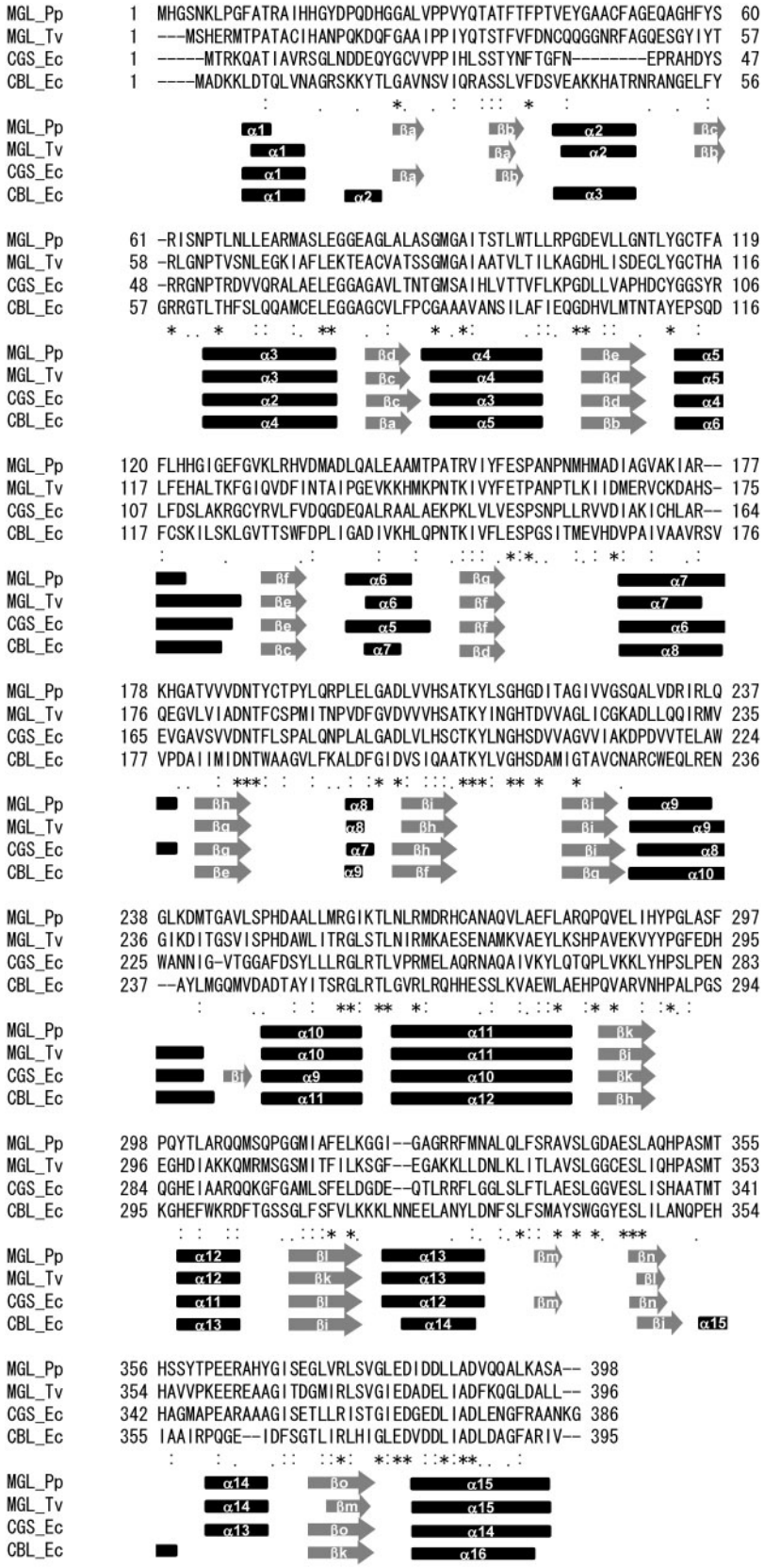

Fig. 5. **Structure-based alignment of MGL_Pp (MGL from *P. putida*) with MGL_tv (MGL from *T. vaginalis*, 1E5F), CGS_Ec (CGS from *E. coli*, 1CS1) and CBL_Ec (CBL from *E. coli*, 1CL1).** Helices and strands appear as cylinders and arrows. Conserved residues are shown with asterisks, homologues with dots and colons.

(*32*), the solved crystal structure of MGL_Pp shows remarkable structural similarity of this enzyme to aminotransferase, subclass I, and the cystathionine β-lyase subclass (Fig. 5). The diagnostic tetramer formation functions as a factor to maintain the active dimer (Fig. 2). The N-terminal region (residual 1–63), which plays an important role in the formation of the active dimer and substrate recognition, is very flexible in MGL_Pp (Figs. 2 and 3). Residues involved in anchoring PLP are essentially optimized for each reaction. Specificity stems from the steric and non-electrostatic accessibility of the active sites rather than the exchange of catalytically important residues (Arg61*, Tyr114 and Cys116) (*27*, *28*). Although MGL_Pp shows relatively low sequence identity to other γ-family enzymes, CBL_Ec, CGS_Ec, and MGL_Tv contain folds that are very similar to that of MGL_Pp. Without exception, the active-site geometries of these γ-family enzymes are mostly conserved. The structural homologies strengthen the suggestion that the PLP enzymes of the γ-family, with various functions, evolved from a common ancestral protein. High-resolution structures, as exemplified by the present work, should prove beneficial in the design of specific antitumour agents, targeting altered methionine metabolism and altered methylation in tumour cells (*34*, *37*).

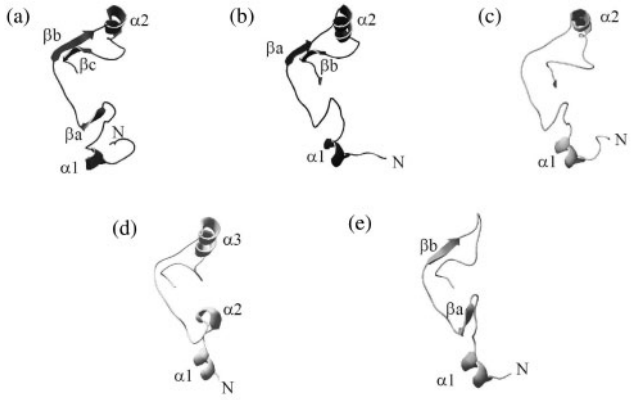

Fig. 6. **Comparison of N-terminus of MGL_Pp (a, residues 1-63) with those of MGL_Tv (b, residues 4-61), MGL_Cf (c, residues 2-63), CBL_Ec (d, residues 5–60) and CGS_Ec (e, residues 3-51).** Pay attention to the differences between the crystallography of CBL (1CL1) and CGS (1CS1) and the previous reports (*24*, *27*).

REFERENCES

1. Vermeij, P. and Kertesz, M.A. (1999) Pathways of assimilative sulfur metabolism in *Pseudomonas putida*. *J. Bacteriol.* **181**, 5833–5837
2. Inoue, H., Inagaki, K., Eriguchi, S., Tamura, T., Esaki, N., Soda, K., and Tanaka, H. (1997) Molecular characterization of the *mde* operon involved in L-methionine catabolism of *Pseudomonas putida*. *J. Bacteriol.* **179**, 3956–3962
3. Tanaka, H., Esaki, N., and Soda, K. (1977) Properties of L-methionine γ-lyase from *Pseudomonas ovalis*. *Biochemistry* **16**, 100–106
4. Lockwood, B.C. and Coombs, G.H. (1991) Purification and characterization of methionine γ-lyase from *Trichomonas vaginalis*. *Biochem. J.* **279**, 675–682
5. Tokoro, M., Asai, T., Kobayashi, S., Takeuchi, T., and Nozaki, T. (2003) Identification and characterization of two isoenzymes of methionine γ-lyase from *Entamoeba histolytica*: a key enzyme of sulfur-amino acid degradation in an anaerobic parasitic protist that lacks forward and reverse trans-sulfuration pathways. *J. Biol. Chem.* **278**, 42717–42727
6. Nakayama, T., Esaki, N., Lee, W.J., Tanaka, I., Tanaka, H., and Soda, K. (1984) Purification and properties of L-methionine γ-lyase from *Aeromonas* sp. *Agric. Biol. Chem.* **48**, 2367–2369
7. Manukhov, I.V., Mamaeva, D.V., Rastorguev, S.M., Faleev, N.G., Morozova, E.A., Demidkina, T.V., and Zavilgelsky, G.B. (2005) A gene encoding L-methionine γ-lyase is present in *Enterobacteriaceae* family genomes: identification and characterization of *Citrobacter freundii* L-methionine γ-lyase. *J. Bacteriol.* **187**, 3889–3893
8. Amarita, F., Yvon, M., Nardi, M., Chambellon, E., Delettre, J., and Bonnarme, P. (2004) Identification and functional analysis of the gene encoding methionine γ-lyase in *Brevibacterium linens*. *Appl. Environ. Microbiol.* **70**, 7348–7354
9. Yoshimura, M., Nakano, Y., Yamashita, Y., Oho, T., Saito, T., and Koga, T. (2000) Formation of methyl mercaptan from L-methionine by *Porphyromonas gingivalis*. *Infect. Immun.* **68**, 6912–6916
10. Fukamachi, H., Nakano, Y., Okano, S., Shibata, Y., Abiko, Y., and Yamashita, Y. (2005) High production of methyl mercaptan by L-methionine-alpha-deamino-gamma-mercaptomethane lyase from *Treponema denticola*. *Biochem. Biophys. Res. Commun.* **331**, 127–131
11. Miki, K., Xu, M., An, Z., Wang, X., Yang, M., Al-Refaie, W., Sun, X., Baranov, E., Tan, Y., Chishima, T., Shimada, H., Moossa, A.R., and Hoffman, R.M. (2000) Survival efficacy of the combination of the methioninase gene and methioninase in a lung cancer orthotopic model. *Cancer Gene Ther.* **7**, 332–338
12. Yamamoto, N., Gupta, A., Xu, M., Miki, K., Tsujimoto, Y., Tsuchiya, H., Tomita, K., Moossa, A.R., and Hoffman, R.M. (2003) Methioninase gene therapy with selenomethionine induces apoptosis in bcl-2-overproducing lung cancer cells. *Cancer Gene Ther.* **10**, 445–450
13. Tan, Y., Sun, X., Xu, M., Tan, X., Sasson, A., Rashidi, B., Han, Q., Tan, X., Wang, X., An, Z., Sun, F.X., and Hoffman, R.M. (1999) Efficacy of recombinant methioninase in combination with cisplatin on human colon tumors in nude mice. *Clin. Cancer Res.* **5**, 2157–2163
14. Tan, Y., Xu, M., Tan, X., Wang, X., Saikawa, Y., Nagahama, T., Sun, X., Lenz, M., and Hoffman, R.M. (1997) Overexpression and large-scale production of recombinant L-methionine-α-deamino-γ-mercaptomethane-lyase for novel anticancer therapy. *Protein Expr. Purif.* **9**, 233–245
15. Miki, K., Al-Refaie, W., Xu, M., Jiang, P., Tan, Y., Bouvet, M., Zhao, M., Gupta, A., Chishima, T., Shimada, H., Makuuchi, M., Moossa, A.R., and Hoffman, R.M. (2000) Methioninase gene therapy of human cancer cells is synergistic with recombinant methioninase treatment. *Cancer Res.* **60**, 2696–2702
16. Tan, Y., Sun, X., Xu, M., An, Z., Tan, X., Han, Q., Miljkovic, D.A., Yang, M., and Hoffman, R.M. (1998) Polyethylene glycol conjugation of recombinant methioninase for cancer therapy. *Protein Expr. Purif.* **12**, 45–52
17. Sun, X., Yang, Z., Li, S., Tan, Y., Zhang, N., Wang, X., Yagi, S., Yoshioka, T., Takimoto, A., Mitsushima, K., Suginaka, A., Frenkel, E.P., and Hoffman, R.M. (2003) In vivo efficacy of recombinant methioninase is enhanced by the combination of polyethylene glycol conjugation and pyridoxal 5′-phosphate supplementation. *Cancer Res.* **63**, 8377–8383
18. Yang, Z., Sun, X., Li, S., Tan, Y., Wang, X., Zhang, N., Yagi, S., Takakura, T., Kobayashi, Y., Takimoto, A., Yoshioka, T., Suginaka, A., Frenkel, E.P., and

Hoffman, R.M. (2004) Circulating half-life of PEGylated recombinant methioninase holoenzyme is highly dose dependent on cofactor pyridoxal-5′-phosphate. *Cancer Res.* **64**, 5775–5778
19. Yang, Z., Wang, J., Lu, Q., Xu, J., Kobayashi, Y., Takakura, T., Takimoto, A., Yoshioka, T., Lian, C., Chen, C., Zhang, D., Zhang, Y., Li, S., Sun, X., Tan, Y., Yagi, S., Frenkel, E.P., and Hoffman, R.M. (2004) PEGylation confers greatly extended half-life and attenuated immunogenicity to recombinant methioninase in primates. *Cancer Res.* **64**, 6673–6678
20. Motoshima, H., Inagaki, K., Kumasaka, T., Furuichi, M., Inoue, H., Tamura, T., Esaki, N., Soda, K., Tanaka, N., Yamamoto, M., and Tanaka, H. (2000) Crystal structure of the pyridoxal 5′-phosphate dependent L-methionine γ-lyase from *Pseudomonas putida*. *J. Biochem.* **128**, 349–354
21. Mamaeva, D.V., Morozova, E.A., Nikulin, A.D., Revtovich, S.V., Nikonov, S.V., Garber, M.B., and Demidkina, T.V. (2005) Structure of *Citrobacter freundii* L-methionine γ-lyase. *Acta. Cryst.* **F61**, 546–549
22. Takakura, T., Mitsushima, K., Yagi, S., Inagaki, K., Tanaka, H., Esaki, N., Soda, K., and Takimoto, A. (2004) Assay method for antitumor L-methionine γ-lyase: comprehensive kinetic analysis of the complex reaction with L-methionine. *Anal. Biochem.* **327**, 233–240
23. Takakura, T., Ito, T., Yagi, S., Notsu, Y., Itakura, T., Nakamura, T., Inagaki, K., Esaki, N., Hoffman, R.M., and Takimoto, A. (2006) High-level expression and bulk crystallization of recombinant L-methionine γ-lyase, an anticancer agent. *Appl. Microbiol. Biotechnol.* **70**, 183–192
24. Clausen, T., Huber, R., Laber, B., Pohlenz, H.D., and Messerschmidt, A. (1996) Crystal structure of the pyridoxal-5′-phosphate dependent cystathionine β-lyase from *Escherichia coli* at 1.83 Å. *J. Mol. Biol.* **262**, 202–224
25. Johnston, M., Jankowski, D., Marcotte, P., Tanaka, H., Esaki, N., Soda, K., and Walsh, C. (1979) Suicide inactivation of bacterial cystathionine γ-synthase and methionine γ-lyase during processing of L-propargylglycine. *Biochemistry* **18**, 4690–4701
26. Eliot, A.C. and Kirsch, J.F. (2002) Modulation of the internal aldimine p*Ka*'s of 1-aminocyclopropane-1-carboxylate synthase and aspartate aminotransferase by specific active site residues. *Biochemistry* **41**, 3836–3842
27. Clausen, T., Huber, R., Prade, L., Wahl, M.C., and Messerschmidt, A. (1998) Crystal structure of *Escherichia coli* cystathionine γ-synthase at 1.5 Å resolution. *EMBO J.* **17**, 6827–6838
28. Hayashi, H., Inoue, Y., Kuramitsu, S., Morino, Y., and Kagamiyama, H. (1990) Effects of replacement of tryptophan-140 by phenylalanine or glycine on the function of *Escherichia coli* aspartate aminotransferase. *Biochem. Biophys. Res. Commun.* **167**, 407–412
29. Inoue, H., Inagaki, K., Adachi, N., Tamura, T., Esaki, N., Soda, K., and Tanaka, H. (2000) Role of tyrosine 114 of L-methionine γ-lyase from *Pseudomonas putida*. *Biosci. Biotechnol. Biochem.* **64**, 2336–2343
30. Nakayama, T., Esaki, N., Tanaka, H., and Soda, K. (1988) Chemical modification of cysteine residues of L-methionine γ-lyase. *Agric. Biol. Chem.* **52**, 177–183
31. Messerschmidt, A., Worbs, M., Steegborn, C., Wahl, M.C., Huber, R., Laber, B., and Clausen, T. (2003) Determinants of enzymatic specificity in the Cys-Met-metabolism PLP-dependent enzymes family: crystal structure of cystathionine γ-lyase from yeast and intrafamiliar structure comparison. *J. Biol. Chem.* **384**, 373–386
32. Inoue, H., Inagaki, K., Sugimoto, M., Esaki, N., Soda, K., and Tanaka, H. (1995) Structural analysis of the L-methionine γ-lyase gene from *Pseudomonas putida*. *J. Biochem.* **117**, 1120–1125
33. Dias, B. and Weimer, B. (1998) Purification and characterization of L-methionine γ-lyase from *Brevibacterium linens* BL2. *Appl. Environ. Microbiol.* **64**, 3327–3331
34. Hoffman, R.M. (1984) Altered methionine metabolism, DNA methylation and oncogene expression in carcinogenesis: a review and synthesis. *Biochim. Biophys. Acta* **738**, 49–87
35. Cheah, M.S., Wallace, C.D., and Hoffman, R.M. (1984) Hypomethylation of DNA in human cancer cells: a site-specific change in the *c-myc* oncogene. *J. Natl. Cancer Inst.* **73**, 1057–1065
36. Diala, E.S., Cheah, M.S., Rowitch, D., and Hoffman, R.M. (1983) Extent of DNA methylation in human tumor cells. *J. Natl. Cancer Inst.* **71**, 755–764
37. Mecham, J.O, Rowitch, D, Wallace, C.D, Stern, P.H, Wallace, C.D, and Hoffman, R.M (1983) The metabolic defect of methionine dependence occurs frequently in human tumor cell lines. *Biochem. Biophys. Res. Commun* **117**, 429–434